

## THE S-BAND BEACON RECEIVER FOR THE MIDCOURSE SPACE EXPERIMENT

The Applied Physics Laboratory has developed a space-based system, called the S-band Beacon Receiver, to perform high-resolution angle tracking of cooperative targets for the Midcourse Space Experiment program. During its five-year on-orbit lifetime, the S-band Beacon Receiver must track targets that emit 4 W of S-band beacon power from as far away as 8000 km to an accuracy of  $\pm 0.1^\circ \times \pm 0.1^\circ$  over  $\pm 3^\circ \times \pm 3^\circ$  about boresight. This article describes the Beacon Receiver system and the design features required to achieve the performance specifications.

### INTRODUCTION

The Midcourse Space Experiment (MSX) program provides a multisensor capability for collecting background, target detection, and tracking phenomena data required for the Theater Missile Defense, Brilliant Eyes, and Ground-Based Surveillance and Tracking systems.<sup>1</sup> A high-priority requirement of the program is to characterize various space targets using optical sensors onboard the MSX spacecraft. However, since some of the sensors have a narrow field of view, open-loop pointing of the sensors toward point targets is difficult and risky. The Laboratory developed the S-band Beacon Receiver to provide for acquisition and closed-loop angle tracking of the targets. During operation, the Beacon Receiver precise-target angle measurements are transmitted to the MSX onboard tracking processor, which then commands the spacecraft attitude system to orient the scientific sensors toward the targets, thereby allowing for reliable achievement of the MSX data collection objectives.

Although the Beacon Receiver design is based on well-known phase-comparison monopulse principles, this article will show that the Beacon Receiver development effort required several design innovations to meet all requirements. The precision required is less than 1% of the diffraction limit for the Beacon Receiver antenna array, which is a tight requirement for monopulse systems. That performance must be achieved at large off-boresight angles, precluding a null-steering system. To achieve the narrow system-noise bandwidths necessary for meeting the performance requirements, the Beacon Receiver has extensive capabilities for digital signal processing, as well as a 600-MHz gallium arsenide direct digital synthesizer (DDS) for highly agile and highly precise synthesis of the local oscillator signals. Digital beam-forming and onboard calibration coincident with tracking operations were needed to assure that the Beacon Receiver meets the performance specifications over the temperature, signal strength, and frequency ranges at all off-boresight angles and throughout the mission life-

time. Onboard calibration of the receiver electronics, cabling, and antenna feed assemblies is performed by tracking a pilot-tone signal that is generated by the Beacon Receiver synchronously with the local oscillator signals and injected at the vertex of each antenna reflector. The potential need for target acquisition at large off-boresight angles led to the addition of an amplitude-comparison monopulse mode for acquisition and resolution of the interferometer grating lobes inherent in the phase-comparison monopulse techniques. Finally, the requirement for a deployable, lightweight, yet rigid and thermally stable mechanical structure led to incorporation of an antenna array "bench" made of a graphite epoxy composite material.

### BEACON RECEIVER REQUIREMENTS

During its five-year orbital mission, the Beacon Receiver must acquire cooperative targets with an initial pointing uncertainty of  $\pm 5^\circ \times \pm 5^\circ$  at a range of up to 8000 km and track them with a  $\pm 0.1^\circ \times \pm 0.1^\circ$  residual rms error. Once per second, the Beacon Receiver angle measurements will be transmitted to the MSX tracking processor, which commands the attitude processor to orient the spacecraft toward the target. Figure 1 illustrates the system concept. Each target beacon emits more than 1 W of S-band beacon carrier power in the frequency range from 2200 to 2270 MHz. A minimum of 4 W of beacon power is required for acquisition and tracking of targets at the maximum 8000-km range. The target beacon requirements are summarized in Table 1. Table 2 lists the Beacon Receiver performance requirements for beacons specified in Table 1. Table 3 lists the physical, power, and thermal requirements of the Beacon Receiver.

The Beacon Receiver coordinates are referred to as azimuth and elevation throughout this article to be consistent with terminology established in the MSX program. However, the Beacon Receiver does not measure azimuth and elevation in the usual sense. Figure 2 defines the



**Figure 1.** The Midcourse Space Experiment (MSX) S-band Beacon Receiver system concept. The Beacon Receiver acquires and tracks cooperative space targets to less than 0.1° error over a 10° field of view at ranges to 8000 km. The sum beam (formed by summing the signal received by each of the four Beacon Receiver channels) is used for detection and frequency track. The difference beam (formed by differencing pairs of signals) is used for monopulse angle measurements. Both beams are electronically steered so that the target is positioned on the null of the difference beam.

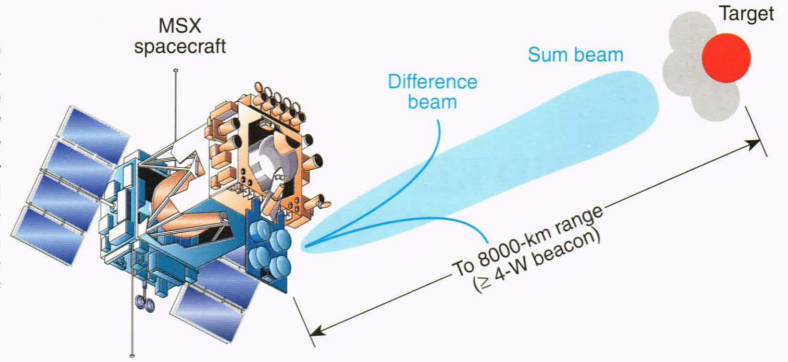


**Table 1.** Target beacon requirements.

Frequency	2200 to 2270 MHz
Format	Continuous wave or residual carrier meeting power requirements
RF carrier power	1–12 W
Antenna gain	> –10 dB relative to an isotropic radiator over 50% of the pattern
Antenna polarization	Nominally linear, minimum axial ratio of 10 dB

**Table 2.** Beacon Receiver performance requirements for beacons specified in Table 1.

Field of regard	$\pm 5^\circ \times \pm 5^\circ$
Maximum RMS angle error	$\pm 0.1^\circ \times \pm 0.1^\circ$ for target within $\pm 3^\circ \times \pm 3^\circ$ , $\pm 0.5^\circ \times \pm 0.5^\circ$ for target within $\pm 5^\circ \times \pm 5^\circ$ but not within $\pm 3^\circ \times \pm 3^\circ$
Maximum acquisition time	15 s
Grating lobe ambiguity	Target off-boresight angle will not be ambiguously reported due to grating-lobe ambiguity
Maximum range	8000 km (requires 4-W beacon) 6000 km (requires 2-W beacon) 4000 km (requires 1-W beacon)
Minimum range	300 km
Initial frequency uncertainty	$\pm 100$ kHz

coordinate system used. As shown, the Beacon Receiver actually outputs the complement of the angle included between the target direction vector and each of two axes mapped into the MSX coordinate system. The nominal Beacon Receiver angles are given mathematically as

$$\text{azimuth} = \arcsin(\hat{\mathbf{p}} \cdot \hat{\mathbf{y}})$$

and

$$\text{elevation} = \arcsin(\hat{\mathbf{p}} \cdot \hat{\mathbf{z}}),$$

**Table 3.** Physical, power, and thermal requirements of the Beacon Receiver.

Size	
Antenna assembly	114 cm × 157 cm × 33 cm
First IF electronics assembly	53 cm × 35 cm × 5 cm
Main electronics assembly	80 cm × 41 cm × 28 cm
Weight	
Antenna assembly	40.9 kg
First IF electronics assembly	9.2 kg
Main electronics assembly	<u>33.2 kg</u>
Total	83.3 kg
Thermal	
Antenna assembly	
Operating range	–50 to –20°C
Survival range	–60 to +40°C
First IF electronics assembly	
Operating range	–50 to –20°C
Survival range	–60 to +40°C
Main electronics assembly	
Operating range	–5 to +66°C
Survival range	–15 to +71°C
Nominal power dissipation	
Antenna assembly	5.5 W
First IF electronics assembly	2.3 W
Main electronics assembly	<u>61.0 W</u>
Total	68.8 W

where  $\hat{\mathbf{p}}$  is a unit vector in the direction of the target,  $\hat{\mathbf{y}}$  is a unit vector in the direction of the spacecraft +y-axis, and  $\hat{\mathbf{z}}$  is a unit vector in the direction of the spacecraft +z-axis. However, because the Beacon Receiver antenna assembly must be deployed on-orbit, the actual Beacon Receiver boresight will not align exactly with the spacecraft +x-axis. The Beacon Receiver boresight will be mapped to the MSX +x-axis soon after launch, and the conversion from Beacon Receiver coordinates to MSX coordinates will thereafter be done in real time by the MSX spacecraft tracking processor.



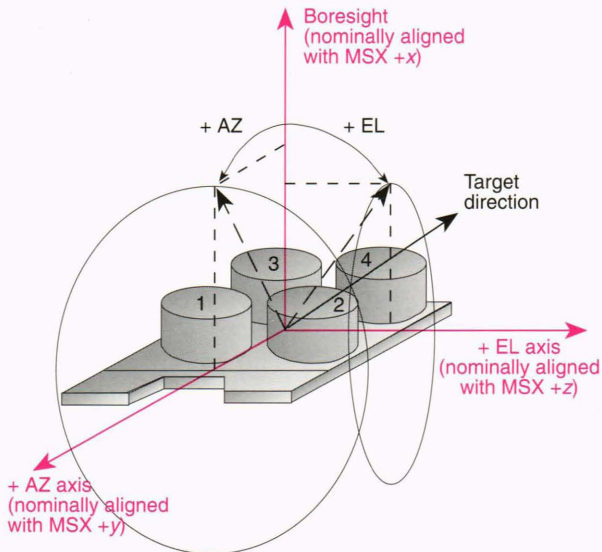


**Figure 2.** Definition of the azimuth (AZ) and elevation (EL) coordinates with respect to the spacecraft coordinates for the Midcourse Space Experiment (MSX) Beacon Receiver.

## SYSTEM PERFORMANCE CONSIDERATIONS

The Beacon Receiver is a passive angle-tracking system. It needs no transmitter because the targets are cooperative and under MSX project control, and because range measurements are not required. An active radar design was rejected because the combination of antenna size and transmitter power needed to illuminate the target sufficiently would have been prohibitively expensive for a spacecraft. S-band radiation was selected because of the availability of beacons and antennas for the targets. The frequency range was narrowed to 2200 to 2270 MHz to avoid interference with the 2282.5-MHz downlink signal radiated by the MSX spacecraft communication system at a power level of 4 W.

Phase-comparison monopulse techniques are used by the Beacon Receiver to derive the high-precision angle measurements. In phase-comparison monopulse systems, the target off-boresight angle is estimated by comparing the phase of a sinusoidal signal as received at several antenna elements in an array of coaligned antennas.<sup>2</sup> Figure 3 illustrates the phase-comparison monopulse concept in one dimension and shows that a spatial angle offset,  $\phi$ , from boresight of the two antenna elements results in a received carrier phase difference,  $\theta$ , of

$$\theta(\text{rad}) = (2\pi S/\lambda) \sin \phi,$$

where  $S$  is the separation between the two antenna phase centers and  $\lambda$  is the beacon radiation free-space wavelength. The Beacon Receiver system receives signals with wavelengths from 13.64 to 13.22 cm and has a square array of four antenna elements on 60.96-cm centers. For small angles where  $\sin \phi \approx \phi$ , there is an angle conversion factor of  $2\pi S/\lambda \approx 28.5$  between the pointing (spatial) angle and channel-to-channel electrical phase angle. Measurement of the spatial angle to  $0.1^\circ$  thus requires measurement of channel-to-channel electrical phase angles to approximately  $2.85^\circ$ .

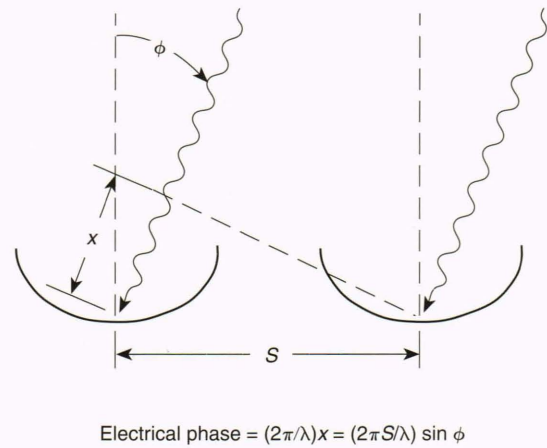


**Figure 3.** Phase-comparison monopulse concept. The channel-to-channel electrical phase is related to the spatial angle,  $\phi$ , the dish separation,  $S$ , and the electrical free-space wavelength,  $\lambda$ , as shown.

Since the phase of a sinusoidal signal can only be measured modulo  $2\pi$ , ambiguities arise for spatial angles that would cause a greater than  $2\pi$  phase difference, that is, for  $\phi > \arcsin(\lambda/S)$ . This ambiguity is manifested as a family of interferometric grating lobes (similar to antenna pattern side lobes) with a lobe spacing of  $\phi = \arcsin(\lambda/S) \approx 0.22$  rad or approximately  $12.6^\circ$  for the Beacon Receiver. Figure 4 shows the sum-beam antenna pattern for a beam at the array boresight, including the main lobe and adjacent grating lobes as adjusted by the pattern of each antenna element. Because of the grating lobes, targets outside of  $\pm 6.3^\circ \times \pm 6.3^\circ$  about boresight would be interpreted as being inside this area when using phase-comparison monopulse techniques. Even though these targets would be outside the specified acquisition range of the instrument, this situation arises under certain scenarios. The possibility of deriving erroneous data for ambiguous targets is great enough that a means was devised for resolving grating-lobe ambiguities.

To resolve the phase-comparison monopulse grating lobes, the Beacon Receiver antenna elements were tilted slightly away from the array center, allowing for the addition of a low-resolution, amplitude-comparison monopulse mode of operation. Amplitude-comparison monopulse systems derive off-boresight angle measurements from signal-level differences as measured in several overlapping, but not coaligned, antenna beams.<sup>2</sup>

The receiver electronics were designed to provide a worst-case signal-to-noise ratio (SNR) of 10 dB in the processing bandwidth for the combined signal from the four channels at the extremes of range and beacon power over the  $\pm 3^\circ \times \pm 3^\circ$  high-resolution field of view. This SNR is the minimum that will allow for reliable acquisition and tracking of the signal. The link SNR for the Beacon Receiver can be given as follows:

$$\begin{aligned} \text{SNR} &= P_r/N, \\ &= (P_t G_t G_r / L) / (kTB), \end{aligned}$$

or



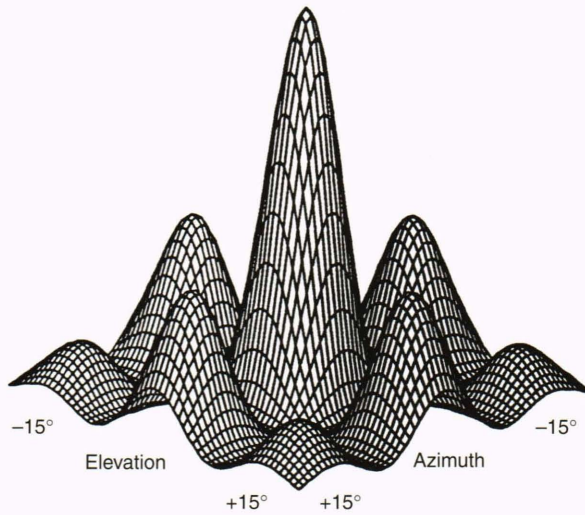


**Figure 4.** Beacon Receiver sum-beam grating-lobe pattern for a beam electronically steered to the array boresight. The large central lobe is the main lobe for channel-to-channel phase differences of  $-\pi$  to  $+\pi$ . For greater phase differences, a periodic grating-lobe structure results. The grating lobes are attenuated relative to the main lobe owing to the effect of the antenna pattern for each element of the antenna array.

$$\text{SNR}(\text{dB}) = P_t(\text{dB}) + G_t(\text{dB}) + G_r(\text{dB}) - L(\text{dB}) - kTB(\text{dB}),$$

where  $P_r$  is the received power,  $N$  is the noise power in the receiver,  $P_t$  is the transmitted power,  $G_t$  is the transmit antenna gain,  $G_r$  is the receive antenna gain,  $k$  is Boltzmann's constant ( $1.38 \times 10^{-23}$  J/K),  $T$  is the effective system temperature in kelvins,  $B$  is the system bandwidth, and  $L$  is the space loss given by

$$L = (\lambda/4\pi R)^2,$$

where  $\lambda$  is the free-space wavelength of the beacon signal and  $R$  is the range in the same units as  $\lambda$ .

Given the target beacon specifications in Table 1 and the performance requirements in Table 2, the link equation showed that four antennas with 18-dB gain were required. The 3-dB beamwidth associated with an 18-dB gain antenna is approximately  $20^\circ$  wide; this width is a good match with the proposed  $\pm 5^\circ \times \pm 5^\circ$  field of regard. Table 4 shows the Beacon Receiver link budget for a 2-W target at 6000 km, which is slightly worse than a 4-W target at 8000 km. Once worst-case SNR is set by solving the link equation, then the dish spacing can be determined, given the angle conversion factor  $2\pi S/\lambda$  derived in Figure 3. It was found that a square array of four antenna elements on 60.96-cm centers would allow the system requirements to be met. This finding led to  $12.6^\circ$  grating-lobe spacing, which is also compatible with the proposed  $\pm 5^\circ \times \pm 5^\circ$  field of regard. Each dish was skewed away from the center by  $4.25^\circ$  to allow for measurement of the off-boresight angles to better than  $\pm 1^\circ \times \pm 1^\circ$  by amplitude-comparison monopulse techniques, while also defocusing the array for phase-comparison monopulse purposes by a maximum of 0.67 dB throughout the  $\pm 5^\circ \times \pm 5^\circ$  specified field of regard.

**Table 4.** Beacon Receiver link budget, relative to front-end electronics input.

Signal input	
Transmit power	33.0 dBm (2W)
Transmit antenna gain	-10.0 dBi
Space loss <sup>a</sup>	-175.1 dB
Receive antenna array gain <sup>b</sup>	18.8 dB
Pointing loss (at azimuth, elevation = $3.5^\circ, 3.5^\circ$ )	-0.8 dB
Array defocus loss	-0.7 dB
Feed cable loss	-1.0 dB
Filter loss (part of FEE)	0 dB
Total signal power received at FEE input	-135.8 dBm
Noise input	
$k$ (Boltzmann's constant)	$1.38 \times 10^{-23}$ J/K
System temperature at FEE input <sup>c</sup>	304.3 K
Bandwidth	390.625 Hz
Total noise power at FEE input	-147.9 dBm
SNR at FEE input	12.1 dB

Note: FEE = front-end electronics; SNR = signal-to-noise ratio.

<sup>a</sup>Range = 6000 km, frequency = 2250 MHz.

<sup>b</sup>Receive antenna diameter = 45.72 cm, receive antenna efficiency = 65%, off-boresight angle =  $0^\circ$ .

<sup>c</sup>Receive antenna temperature = 146.5 K, receive antenna temperature at FEE = 116.4 K, ambient temperature = 233 K ( $-40^\circ\text{C}$ ), passive temperature at FEE = 48 K, FEE temperature at input = 140 K.

In phase-comparison monopulse systems, phase differences in the receiver electronics result in measurement bias errors and loss of sensitivity. During design and fabrication of the Beacon Receiver, steps were taken to phase match the receiver front-end electronics. However, temperature, frequency, and aging effects will lead to phase misalignments. The Beacon Receiver solves this problem through continuous calibration using an S-band pilot-tone signal injected into each signal path. The frequency and power of the pilot tone are controlled so as to track the incoming signal with a small frequency offset, allowing for simultaneous reception and processing of the pilot tone and the received signal. Channel gain is also calibrated to improve the amplitude-comparison monopulse measurements. The processor maintains a calibration table to correct for known variations in the passive components of the pilot-tone distribution network.

## SYSTEM DESIGN DESCRIPTION

Figure 5 is a block diagram of the Beacon Receiver system. The system has four electronics subsystems: the antenna section, RF/IF electronics section, coherent-frequency generator (CFG) section, and digital processing unit (DPU) section. The electronics sections are mounted on three assemblies: the antenna assembly, first IF assembly, and main electronics assembly. Figure 6 shows photographs of the antenna assembly, first IF assembly, and main electronics assembly. The detailed designs of each of the electronics subsystems are described in the following subsections.



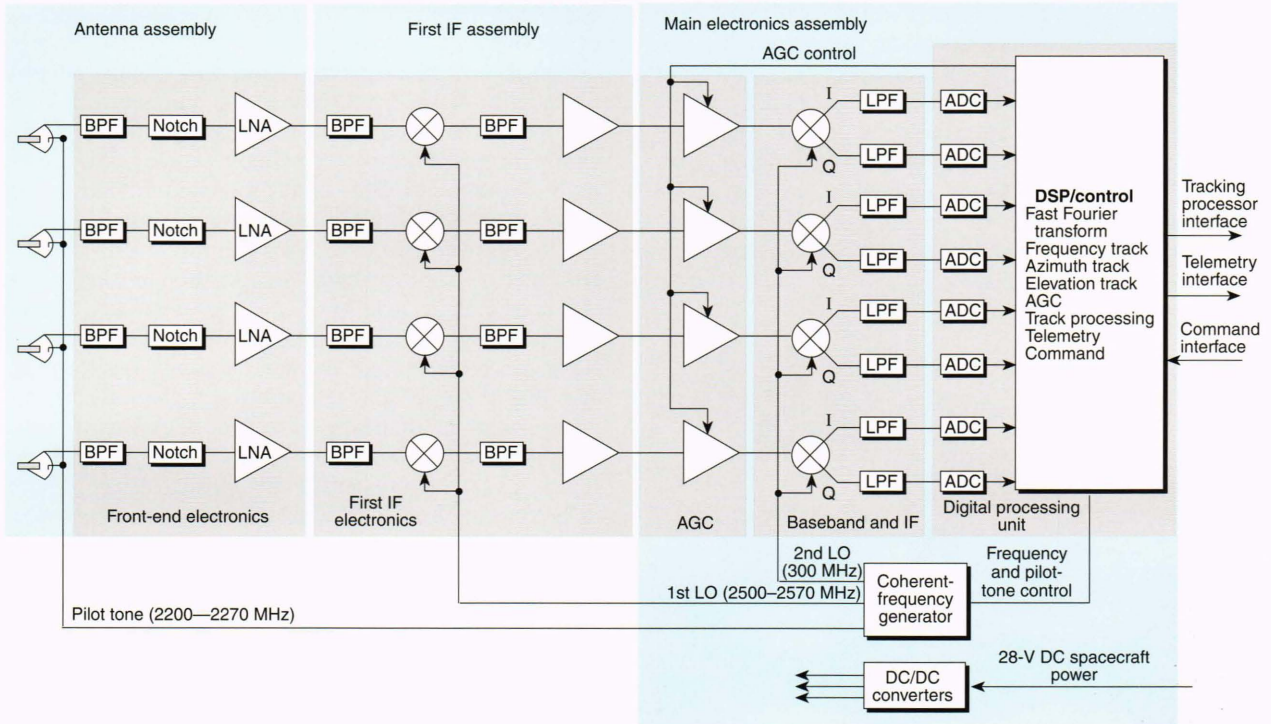


**Figure 5.** Beacon Receiver block diagram. The Beacon Receiver is a four-channel monopulse receiver with four-channel automatic gain control (AGC) and digital beamforming. The Beacon Receiver performs calibration during tracking operations by tracking a pilot-tone signal injected in each antenna dish. The antenna assembly contains the antennas and the front-end electronics segment of the receiver. The first IF assembly contains the first down-conversion stage of the receiver. The main electronics assembly contains the final stage of down-conversion and the AGC attenuators, as well as the coherent-frequency generator, the digital processing unit, and the DC/DC converters. The coherent-frequency generator generates the pilot tone and all local oscillator signals needed to down-convert the received signal plus pilot tone. The digital processing unit performs sampling of the down-converted signal, angle and frequency tracking, and AGC, and provides the interfaces with the MSX spacecraft tracking processor, command system, and telemetry system. The DC/DC converters provide regulated DC power for all of the Beacon Receiver electronics. BPF = bandpass filter, Notch = notch filter, LNA = low-noise amplifier, LPF = low-pass filter, ADC = analog-to-digital converter, I = in-phase, Q = quadrature, LO = local oscillator, DSP = digital signal processing.

## Antenna Section

The antenna section is mounted on the antenna assembly and comprises an array of four parabolic dish antennas along with the provision for pilot-tone distribution and injection. The antenna assembly is hinged so that it can be folded to the side of the spacecraft during launch and then deployed to its operational position after the launch-vehicle fairing has been jettisoned. As described in the System Performance Considerations section, phase monopulse considerations dictated a square array of four 18-dB gain antenna elements on 60.96-cm centers. Circular polarization is required since the target beacons are nominally linear but will have a random orientation.

Several types of antennas were considered for this application, including horns, modified short-backfire antennas, helicones, and small parabolic reflectors. Parabolic antennas are not often used for intermediate gain applications because of difficulty in efficiently illuminating a small reflector without severe aperture blockage. However, previous work at APL has shown that a backfire bifilar helix can give good circularly polarized feed patterns.<sup>3</sup> Since the helix has a relatively small diameter, it causes little aperture blockage.

The antenna design uses an aluminum parabolic reflector with an effective diameter of 45.72 cm and a focal

length of 16 cm. The feed is realized by wrapping two lengths of RG316 coaxial cable onto a cylinder machined with grooves to guide the cables into a bifilar helix geometry that is 2.6975 cm in diameter and has 3.5 turns in an axial length of 11.56 cm. One of the coaxial lines feeds the helix with its center conductor connected to the outer conductor of the opposite coaxial line at the helix end closest to the reflector vertex (a technique sometimes called an "infinite balun"). The outer surfaces of the coaxial cables form the radiating elements of the helix. Impedance matching is achieved by planar conductor pieces soldered to the radial portion of the elements at the feed region. Each antenna dish assembly is right-hand circularly polarized with a boresight gain of 19 dB (1 dB better than the specification), a 3-dB beamwidth of 18°, and side lobes at least 20 dB down from boresight gain.

The pilot tone for each of the four channels could have been injected at the inputs to the front-end electronics to calibrate later stages of the receiver. Such an approach was considered early in the design. However, calculations showed that minor temperature differences among the antennas would result in phase changes in the cables and the feeds that would lead to unacceptable errors in the angle measurements. The antennas and cables therefore had to be included in the calibration path. This setup is



accomplished by injecting the pilot tone via small, bent monopole antennas mounted in the vertex of each parabolic reflector since they provide adequate coupling of the pilot tone to the feed without noticeable degradation to the performance of the reflector antennas. The pilot-tone distribution network introduces a calibration problem because it represents a segment of the calibration path that is not part of the signal path. The pilot-tone distribution network uses temperature-compensated cables and was carefully characterized during integration so

that phase delays could be stored in read-only memory in the DPU's control processor.

Signals reflected from the spacecraft structure have the potential to be received through the antenna side lobes, corrupting the directly received signals and producing multipath phase errors. Experiments were performed to see if cylindrical metal shields mounted around the antennas could significantly reduce the antenna side lobes due to spillover. However, the small size of the antennas prevented a large reduction in radiation in the desired region, and an average of only about 3 dB was achieved. (Shields lined with absorbing material were also tried. However, because their diameter was not much greater than that of the reflectors, and because the reflectors are rather small in diameter in terms of electrical wavelengths, unacceptable reductions in boresight gain resulted, so this approach was abandoned.) The side-lobe reduction benefit of 3 dB was assessed as marginal. However, the antenna performance was not degraded, and the shields proved to be useful in the design of the thermal control system; therefore, the shields were incorporated into the design. The cylindrical shields formed convenient surfaces on which to mount thermal blankets, and radomes were developed to cover the apertures and shade the dish assemblies. The radomes are constructed of an epoxy glass meeting the spacecraft outgassing specifications. They are made thin (approximately 0.075 cm) to minimize electrical effects and are formed into shallow domes for stiffness. Electrically transparent thermal-control paint is applied to their exterior surfaces. The radomes reduce the antenna gain by about 0.3 dB but do not cause an impedance mismatch. Figure 7 is a photograph of the engineering model antenna dish assembly, showing the reflector, feed, and vertex antenna.

From the start of the mechanical design process, it was apparent that it would be difficult to design a deployable structure that would hold the antenna elements in proper alignment under all anticipated thermal conditions. Several designs using traditional materials were considered but failed to yield a solution that could be shown to meet the specifications with adequate design margin. For ex-

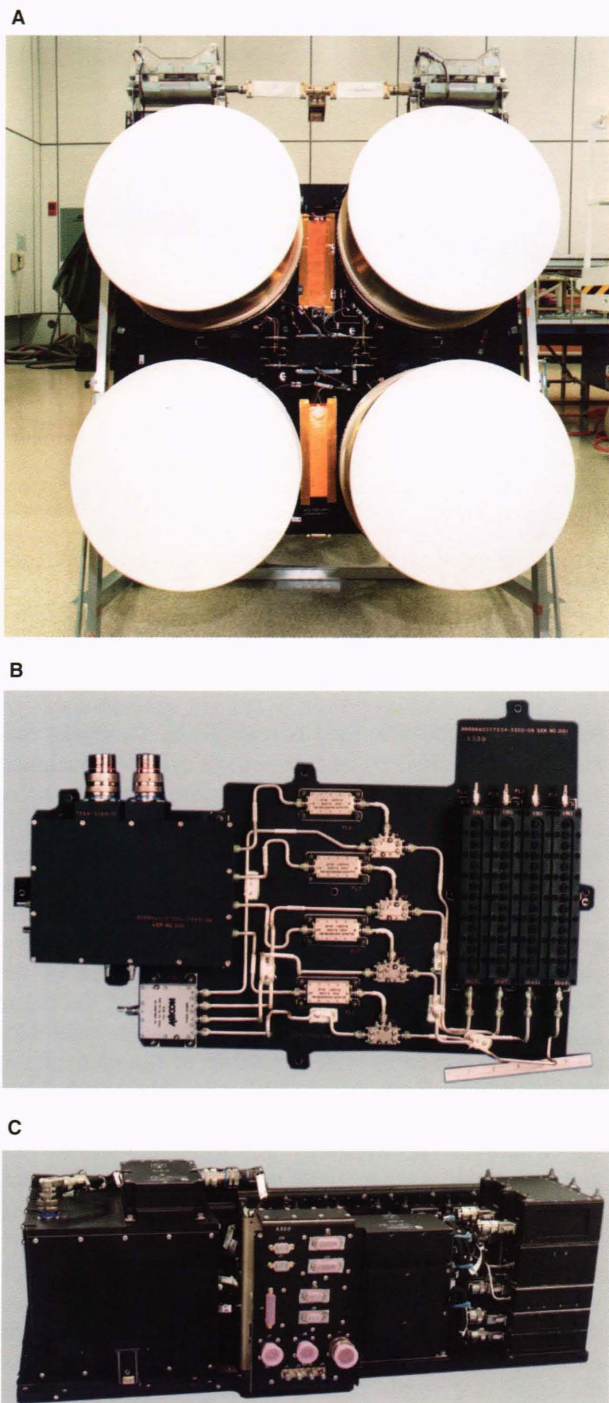


**Figure 6.** Beacon Receiver flight hardware. **A.** Antenna assembly. **B.** First IF assembly. **C.** Main electronics assembly.

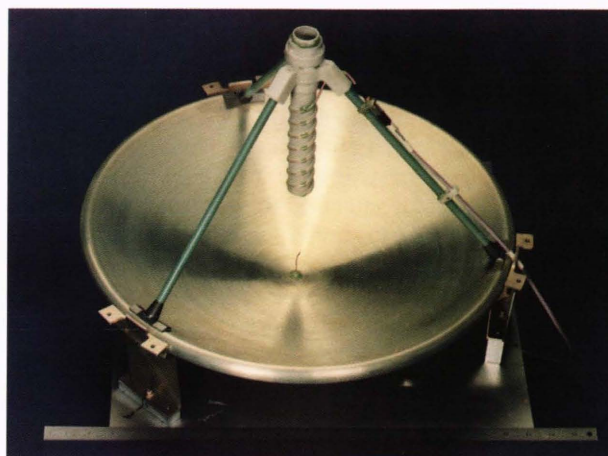


**Figure 7.** Beacon Receiver engineering model antenna dish assembly. The thermal shroud is removed to display the feed assembly at dish focus and pilot-tone injection feed at dish vertex.



ample, finite-element modeling showed that an aluminum honeycomb structure with aluminum struts would exceed the maximum boresight shift specification with a through-deck gradient of less than 2°C. Thermal control methods were considered, but issues of design margin, model confidence, and testability could not be solved. Adjusting the system error budget did not provide adequate relief and introduced problems elsewhere. Loosening the system specification was considered but was found to be unacceptable. However, graphite epoxy composite optical bench structures were being developed for other parts of the MSX spacecraft that exceeded the antenna array requirements for the Beacon Receiver. The graphite epoxy mix can be made such that the coefficient of thermal expansion is effectively zero over the temperature range of interest. Composite Optics, Inc., developed the detailed design and fabricated a graphite epoxy antenna bench that meets specification with a through-deck gradient of over 33°C.

Graphite epoxy was also considered as a material for the dish assemblies, particularly for the reflectors and feed struts. Once the thermal design was established, the effects of thermal distortion of the reflectors and thermally induced displacements of the feeds were analyzed. The predicted temperature distributions for several types of thermal environments were applied to a MacNeal-Schwendler Corp. NASA Structural Analysis Program finite-element model to compute the resulting displacements of the feed and of the reflector surface. The displacements were then used in a modified version of the Numerical Electromagnetics Code-General Reflector Code to determine the changes in received electrical phase. After several design iterations, the errors were reduced to acceptable levels, indicating that the reflectors could be made of spun aluminum and the feed assemblies could be made of fiberglass.<sup>4</sup>

Another numerical modeling procedure was used to estimate the phase errors due to multipath from signals scattered by the spacecraft structure. The structure of the forward end of the spacecraft was modeled for a modified version of the Numerical Electromagnetics Code-Basic Scattering Code using a collection of plates, cylinders, and cone frustums. The results of this study indicate that less than 0.006° of pointing error is to be expected from this source.

### RF/IF Electronics Section

The RF/IF electronics section of the Beacon Receiver provides for filtering, amplification, and down-conversion of the received S-band signals to near baseband. It contains four separate channels, one for each antenna element. Each channel is made up of four components: the front-end electronics, the first IF electronics, an automatic gain control (AGC) module, and a baseband and IF electronics module. Figure 8 is a block diagram of one of the four channels in the RF/IF electronics.

The front-end electronics establishes the SNR for the Beacon Receiver (along with antenna noise and feeder loss), provides gain and selectivity in the 2200- to 2270-MHz band, and rejects the 2282.5-MHz telemetry downlink signal radiated from the MSX spacecraft. To maximize

the SNR, the feeder losses from the antenna feed to the low-noise amplifier (LNA) were minimized by locating the front-end electronics on the antenna assembly and by using low-loss cables. Bandpass and notch filters add some loss but are needed to attenuate interfering signals that can drive the LNA into saturation. The LNA was selected to have minimum noise figure with enough gain to ensure that the system SNR is set by the LNA. The lengths of all cable runs were made to be nominally identical so that the four channels were closely phase-matched; however, they did not have to be exactly identical because the Beacon Receiver is calibrated under operational conditions using the pilot-tone signal. Each LNA output is routed from the antenna assembly over the hinge to the first IF electronics through low-loss coaxial cable.

The first IF electronics section provides for additional filtering and amplification, as well as for down-conversion of the received S-band signal to the 300-MHz IF. The 2500- to 2570-MHz high-side first local oscillator (LO) signal comes from the first LO generator of the CFG section on the main electronics assembly. The width of the IF bandpass filter (5.5 MHz) sets the minimum spacing between target signals. As with the front-end electronics, the lengths of all the S-band cable runs were made nominally identical to provide reasonable phase-matching; residual phasing adjustments are made with software using the pilot tone as a reference. The 300-MHz IF output from each IF amplifier is routed to an AGC attenuator module on the main electronics assembly. The first IF electronics occupies its own assembly located near the antenna assembly on the instrument section of the spacecraft.

Each of the four AGC attenuator modules provides two stages of gain and attenuation. The two attenuators in each module share control lines from the DPU to provide 0 to 63 dB of attenuation in 1-dB steps. The gain-controlled IF output from each AGC attenuator is routed to a baseband and IF electronics module. The four AGC attenuator modules are housed in 16.5 cm × 9.4 cm × 3.8 cm aluminum housings and fit in a stack on the main electronics assembly.

The four baseband and IF electronics modules provide for final amplification and filtering of the IF signals. The received signals are mixed to baseband in the in-phase/quadrature (I/Q) phase detector using the 300-MHz fixed second LO signal from the fixed-frequency synthesizer (FFS) module in the CFG. The I/Q phase detector is a device that develops both the in-phase and quadrature components of the incoming IF signal relative to the second LO. The baseband in-phase and quadrature signals are then amplified, low-pass-filtered to avoid alias problems in the sampling process, and transmitted to the DPU. A test port is provided to allow access to the 300-MHz IF signal just prior to I/Q detection during system calibration and ground testing. The four baseband and IF electronics modules are housed in 15.25 cm × 9.4 cm × 3.8 cm aluminum housings and fit in a stack on the main electronics assembly.

### Coherent-Frequency Generator

The CFG section of the Beacon Receiver provides the first and second LO signals required for the down-conver-



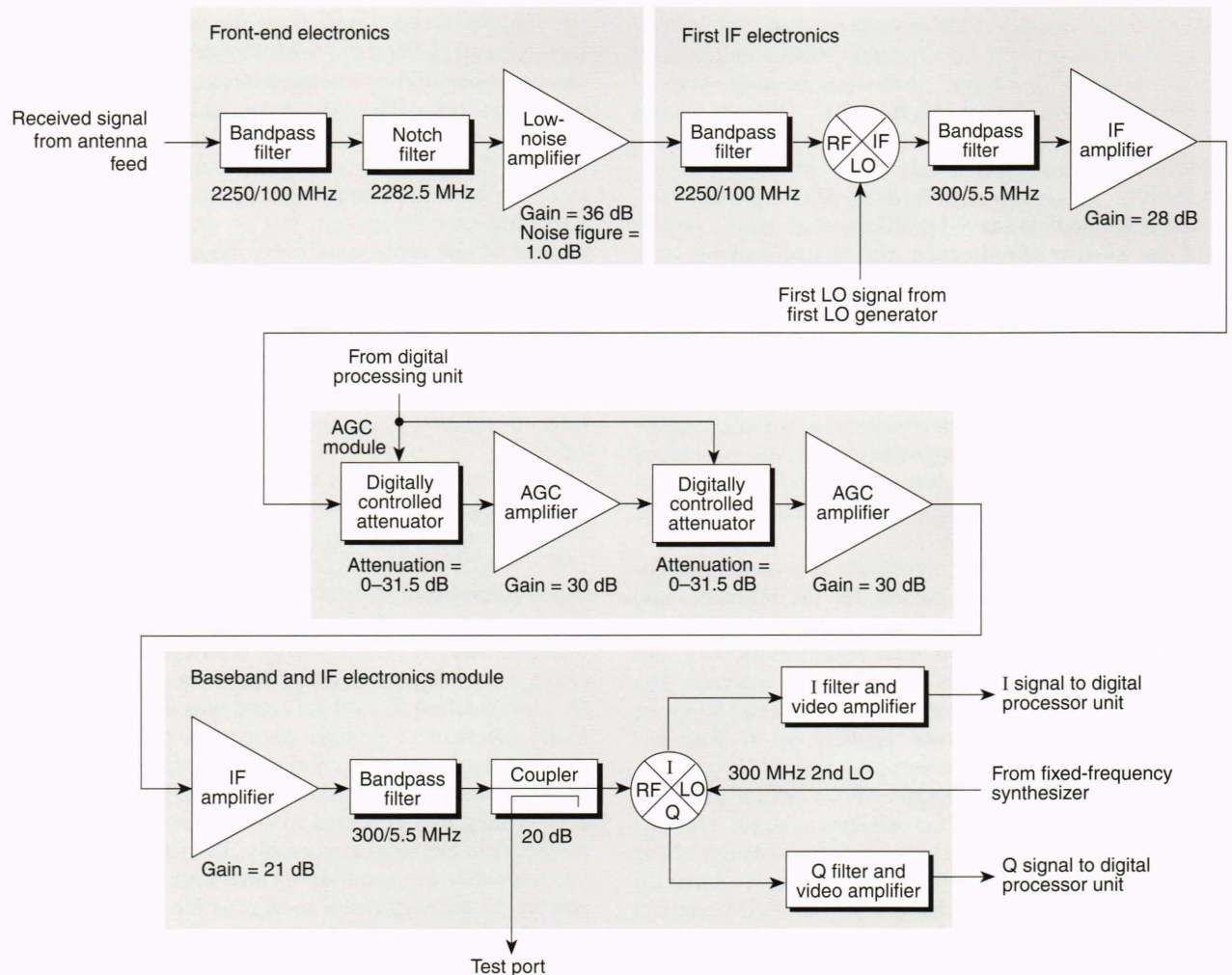


**Figure 8.** Beacon Receiver RF/IF electronics single-channel block diagram. The RF/IF electronics section provides for filtering, amplification, gain control, and down-conversion of the received S-band signals to near baseband. The front end of the RF/IF electronics section is mounted on the antenna assembly deck between the antenna dishes. Down-conversion to the 300-MHz IF is performed in the first IF electronics on the first IF assembly, which is located near the antenna assembly. Automatic gain control (AGC) and the final stage of down-conversion are performed in the AGC modules, the baseband, and IF modules on the main electronics assembly some 15 ft away from the antenna assembly. LO = local oscillator, I = in-phase, Q = quadrature. The numbers given below the bandpass filters are center frequency/bandwidth in megahertz.

sion process and the pilot-tone signal for calibration of the Beacon Receiver. Figure 9 is a block diagram of the CFG. As shown, the CFG contains four modules: the FFS, the DDS, the pilot-tone generator, and the first LO generator. The four modules are housed in separate 11.4 cm  $\times$  15.25 cm aluminum housings with heights varying from 3.8 cm to 5.1 cm, and they fit in a stack on the main electronics assembly.

The FFS is a phase-locked loop that locks to a 5-MHz reference from the MSX spacecraft ultra-stable oscillator and generates the following frequency outputs: 1200 MHz at 10 dBm for the first LO generator, 600 MHz at 8 dBm for the DDS, 300 MHz at 10 dBm for the pilot-tone generator, and 300 MHz at 10 dBm for each of the four baseband and IF electronics modules in the RF/IF electronics section. A voltage-controlled oscillator (VCO) develops the 1200-MHz signal. This signal is divided down to 5 MHz through a divider chain consisting of both

emitter-coupled logic (ECL) and transistor-transistor logic (TTL) digital components. A phase detector compares the phase of the 5-MHz signal with that of the ultra-stable reference. The output of the detector is a voltage that, on average, is proportional to the phase difference between the two 5-MHz signals. This difference voltage is filtered in the loop filter and applied to the VCO, changing the VCO frequency so as to drive the two 5-MHz signals into phase-lock. The divider sequence was chosen so as to provide all frequencies needed. Power amplifiers provide the necessary output drive power. The FFS electronics were implemented on a 0.16-cm-thick G-10 board measuring 7.0 cm  $\times$  14.6 cm. The custom board has 113 g of copper on the component side, as opposed to 56.5 g of copper on the trace side, to help dissipate the 6 W of power generated on the board. Custom heat sinks provide extra heat sinking on the power amplifiers, VCO, ECL dividers, and phase detector.



The DDS is a programmable RF generator that digitally synthesizes sine-wave signals in the 100- to 170-MHz range in approximately 35-Hz steps. The 600-MHz output from the FFS serves as the digital clock for the DDS. Figure 10 is a block diagram of the DDS. The instantaneous signal phase is developed at the phase accumulator, which is a modulo-32 adder. The accumulation rate, and thus the output frequency, are functions of the input clock rate and the frequency-control input. The output of the phase accumulator is an indication of signal phase, which addresses a read-only memory (ROM) that stores one cycle of the output waveform, in this case a sine wave. The sine ROM output is converted to an analog waveform at the digital-to-analog (D/A) converter and then smoothed in the bandpass filter. The DDS was implemented in redundant configuration on two 0.16-cm FR-4 boards mounted back-to-back in an aluminum housing. Each board accommodates a custom hybrid package that includes the gallium arsenide (GaAs), ECL, and TTL digital components in die form. The GaAs components include a Gigabit Logic 10G103 phase accumulator and 14GM048 ROM, and a Triquint Semiconductors TQ6114 D/A convert-

er. The dies were mounted onto a multilayer low-dielectric-constant, low-temperature co-fired "green tape" ceramic substrate. Figure 11 is a top-view photograph of a completed DDS hybrid. Near theoretical performance was achieved by the DDS.<sup>5,6</sup> The output of the DDS is routed to the first LO generator.

The first LO generator module uses the 100- to 170-MHz DDS output and the 1200-MHz FFS output to generate the first LO signal. First, the DDS output is mixed with the 1200-MHz signal to generate a signal in the 1300- to 1370-MHz range, which is then bandpass-filtered to attenuate unwanted harmonics. This signal is then mixed again with the 1200-MHz signal to produce the 2500- to 2570-MHz high-side first LO signal. A very sharp bandpass filter is used to provide over 100-dB rejection of the  $(3 \times \text{LO}) - (2 \times \text{IF})$  intermodulation product. This signal is then amplified and distributed at +16 dBm to the first IF electronics of the RF/IF electronics section on the first IF assembly. A 10-dB coupler is used to develop a +6-dBm output for the pilot-tone generator of the CFG.

The pilot-tone generator module uses the first LO signal from the first LO generator and the 300-MHz second LO signal from the FFS to generate the pilot tone for real-time phase and gain alignment of the Beacon Receiver. To be used during a tracking operation, the pilot-tone power level must be roughly the same as the target beacon signal. A digitally controlled attenuator, using controls received from the DPU, provides level control from at least 10 dB below the minimum expected target signal for acquisition to 10 dB above the maximum expected signal for calibration. This translates to a minimum range of -144 to -104 dBm at the antenna feed or -104 to -64 dBm at the output of the pilot-tone generator. Because it is the product of the first and second LO signals, the pilot tone is received at exactly  $0^\circ$ . However, in order not to be obscured by direct current biases and drifts in the receiver and sampling electronics, the pilot tone is phase-modulated by a  $0^\circ/180^\circ$  modulator synchronized with the sampling operation using control from the DPU.

### Digital Processing Unit and Beacon Receiver Software

The Beacon Receiver DPU section of the main electronics assembly performs signal processing to derive the off-boresight angle measurements from the four channels of baseband I and Q signals provided by the baseband and

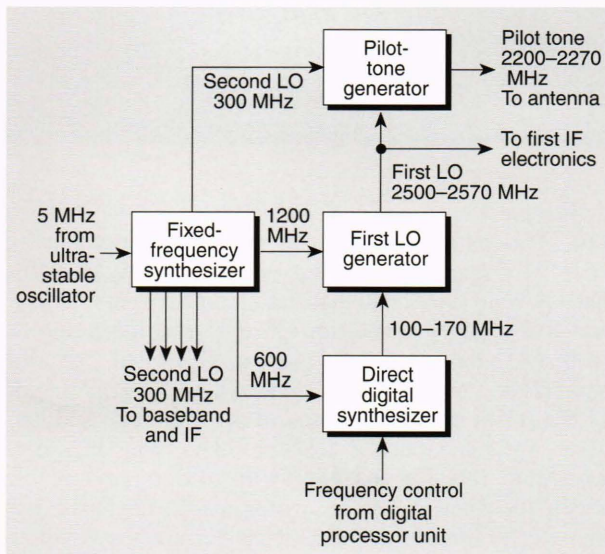


**Figure 9.** Block diagram of the Beacon Receiver coherent-frequency generator on the main electronics assembly, which generates the pilot-tone signal, the first local oscillator (LO) signal, and the second LO signal.

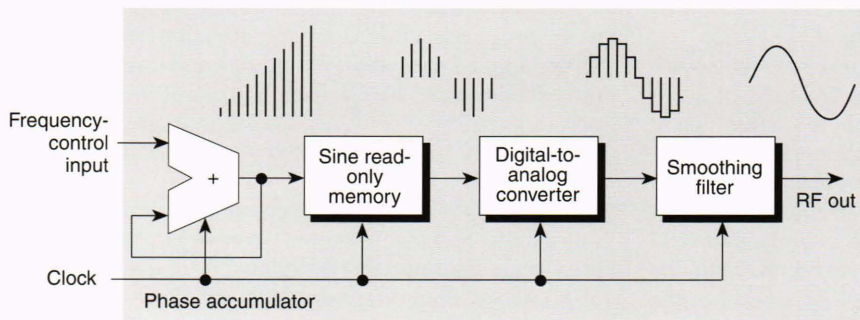
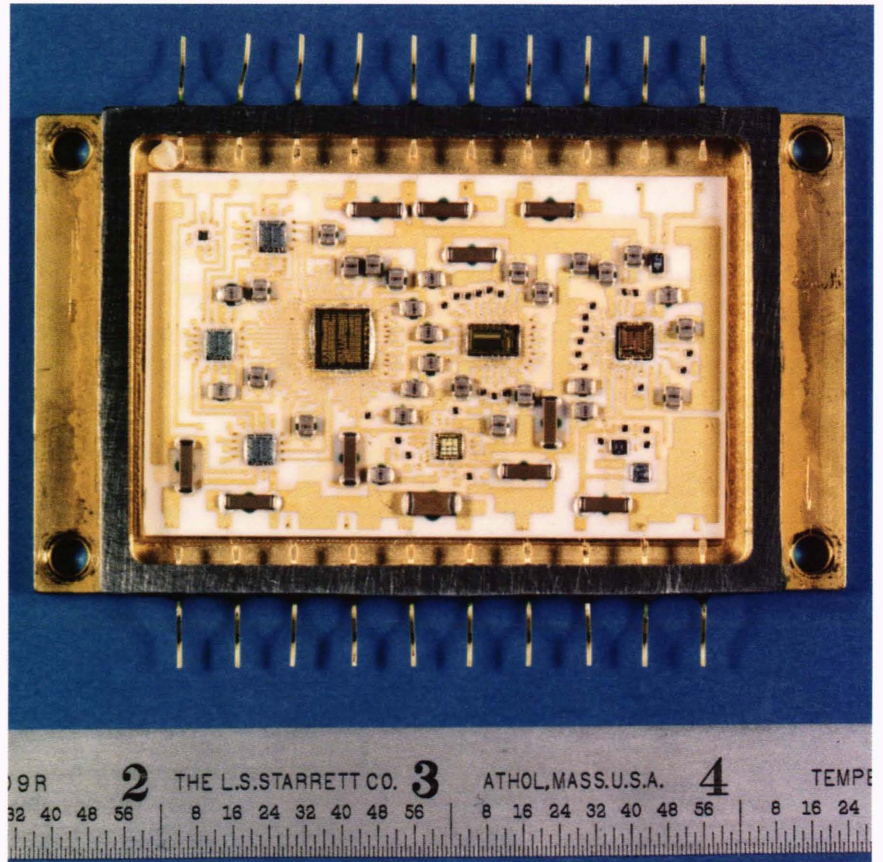


**Figure 10.** Block diagram of the Beacon Receiver direct digital synthesizer. The phase accumulator generates a digital sawtooth sequence with period determined by the frequency-control input. The sine read-only memory contains a digital representation of a single cycle of a sinusoid. It converts the sawtooth sequence to a digital sinusoid, which is then converted to an analog waveform in the digital-to-analog converter and smoothed in a filter.



**Figure 11.** Beacon Receiver direct digital synthesizer (DDS) with lid removed to show the component side of the APL-designed and -fabricated multichip module. The module contains gallium arsenide, emitter-coupled logic, and transistor-transistor logic dies mounted on a multilayer, low-temperature co-fired ceramic substrate to implement a 600-MHz clock rate DDS.



IF electronics modules of the RF/IF electronics section. The DPU also provides for closed-loop frequency tracking and gain control of the received signals through various control interfaces as well as temperature and voltage monitoring. Finally, the DPU provides for command, telemetry, and angle-tracking data interfaces with the rest of the MSX spacecraft. The DPU hardware comprises a card cage containing six 30 cm  $\times$  17.75 cm custom multilayer printed circuit boards and four microprocessors with a combined processing power of over 15 million operations per second. (Simulations on a 25-MHz 80386-based personal computer run at less than 1/100th of the real-time rate.) Figure 12 is a block diagram of the DPU hardware, and Figure 13 is a photograph of the hardware. The Beacon Receiver software contains the codes necessary to implement all signal processing and control functions on the four DPU processors.<sup>7</sup> Implementation of the Beacon Receiver software required development of 3182 lines of "C" code, 806 lines of Analog Devices ADSP-2100 assembly code, and 72 lines of 8086 assembly code.

The analog signal interface board provides for simultaneous sampling of the four I and Q channels at a 50-kHz rate. Blocks of 128 I and Q 8-bit, 2's complement samples are loaded into interface memory on the spectral processor board from each of the four channels. A signal is provided to the pilot-tone generator to control the pilot-tone phase dither so that the phase is only switched between blocks. The sampling is synchronized to the telemetry clock by resetting the sampling control at the once-per-second telemetry major frame rate.

The spectral processor board applies a 128-bit complex fast Fourier transform (FFT) to each of the four I and Q channels every 2.56 ms. This process is equivalent to a narrow-band filter bank that simultaneously provides narrow-band frequency selection (390.625-Hz bin spacing) as well as signal-phase information. The blocks of data samples are "time-domain windowed" before application of the FFT to avoid interaction of the pilot tone and data tones through spectral leakage.<sup>8</sup> (A "window" is a weighting function applied to the data to reduce the spectral leakage by smoothly bringing the data to zero at the interval boundaries.) Real-time performance requirements dictated that the window and FFT algorithms be coded in highly optimized assembly code and executed on two ADPS-2100 programmable digital signal processors running at 20 MHz (5-MHz instruction cycle). The algorithm simultaneously processes two interleaved complex data streams in a single complex, decimation-in-frequency, fixed-point, radix-4 FFT in 1.92 ms. The output of the process is a frequency domain representation of the input sampled data streams with real and imaginary components for each 390.625-Hz bin over a 50-kHz span. The output complex spectra are loaded into an output interface memory to be read by the angle and tracking processor board.

The angle and tracking processor board uses the spectral data to compute target off-boresight angles. During tracking, a calibration is first derived for each data point on the basis of the signal in the pilot-tone bin. Then a beam is digitally formed from the signal in the target bins



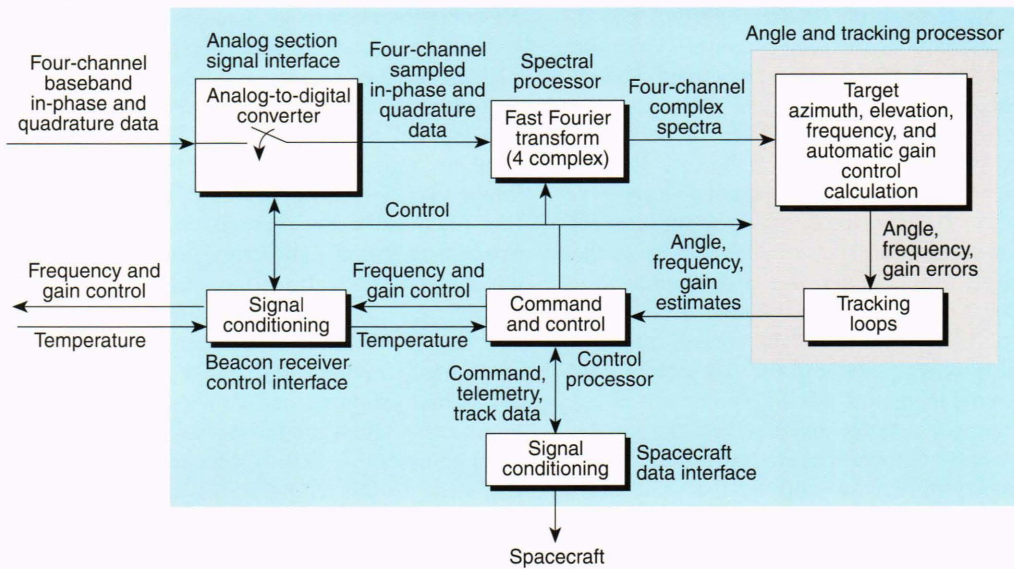


**Figure 12.** Block diagram of the Beacon Receiver digital processing unit (DPU). Received signals are digitized and processed in the DPU on the main electronics assembly. The DPU controls the gain control attenuators, first local oscillator frequency, and pilot-tone frequency, level, and phase. The DPU also receives serial commands from the spacecraft command processor, transmits angle measurements to the spacecraft tracking processor, and transmits serial telemetry to the spacecraft telemetry processor.

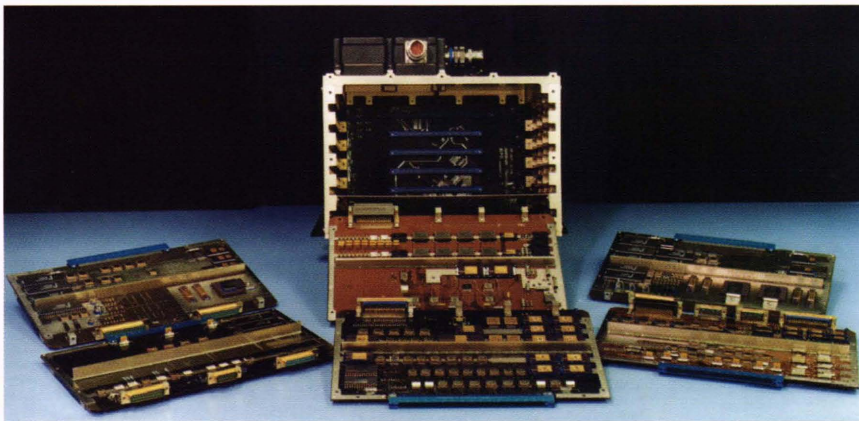


**Figure 13.** Beacon Receiver digital processing unit. Boards are the analog section signal interface board (center), and (counter-clockwise from upper left) the angle and tracking processor board, spacecraft data interface board, control processor board, control interface board, and spectral processor board.

for each channel and digitally steered to the estimated target angles. Phase-comparison monopulse processing derives angle errors that represent the noisy estimate of the difference between the true off-boresight angle and the current beam-pointing direction. A polarization correction is then applied that represents rotation of the antenna phase center as a function of incident linear polarization angle as well as polarization linearity. Finally, these errors are applied to two second-order alpha-beta tracking loops (one for azimuth and one for elevation) that provide smoothed estimates of the off-boresight angles. The tracking-loop bandwidth is programmable and is expected to be about 1 Hz. Amplitude-comparison monopulse is also performed to provide a coarse check for the phase-comparison monopulse angle estimates. If the two estimates vary by more than a set amount, the Beacon Receiver is assumed to have lost lock of the signal or to be locked on a grating lobe. This amount is set by command and is typically about  $5^\circ$ . A coast capability has been implemented that allows the Beacon

Receiver to coast through signal fades by propagating the alpha-beta tracking loops, assuming no error estimate, if the signal power drops below a set level. The angle and tracking processor board also performs frequency tracking so that the pilot tone and the target signal are separated by 12.5 FFT frequency bins or 4882.8125 Hz. This offset allows for greater than 40-dB separation between the two signals while still keeping the target signal frequency low enough to prevent band edge effects from the baseband (pre-sampling) filter. Finally, the angle and tracking processor board allows for independent gain control of each of the four receiver channels and the pilot tone. All tracking-loop outputs are provided to the control processor board. A single 20-MHz ADSP-2100 digital signal processor performs all the signal processing on the angle and tracking processor board.

The control processor board is based on the Harris 80C86RH microprocessor, which is a low-power, radiation-hardened version of the Intel 8086. This board responds to commands received from the spacecraft com-



mand processor via the spacecraft data interface board. The control processor board exercises control over the DPU boards through a control and status data bus. It controls the frequency of the first LO and pilot-tone signals through the frequency control interface between the control interface board and the DDS of the CFG section. The gain of each channel of the Beacon Receiver is controlled via the AGC interfaces between the control interface board and the four AGC attenuator units of the RF/IF electronics section. Finally, the control processor board sets the level of the pilot-tone signal through the pilot-tone control interface between the control interface board and the pilot-tone generator of the CFG section. The tracking loops on the angle and tracking processor board are sampled once per second and used to derive the telemetry and tracking outputs that are transmitted to the spacecraft telemetry processor and to the spacecraft tracking processor, respectively, via the spacecraft data interface board. The control processor also receives Beacon Receiver temperature and voltage data from the control interface board for insertion into the telemetry stream.

The spacecraft data interface board provides interfaces with the spacecraft command processor, tracking processor, and telemetry processor. The Beacon Receiver control interface board provides control interfaces for the Beacon Receiver DDS, AGC attenuator units, and pilot-tone generator. Both boards operate under the control processor but contain controllers based on the Actel ACT-1020 field programmable gate array that provide for autonomous operation of the interfaces. The controllers simplify the control processor interface processing and thus free the control processor for other tasks.

## TESTING AND QUALIFICATION

The Beacon Receiver testing and qualification plan comprises brassboard and breadboard tests, flight hardware subsystem tests, flight hardware system tests, integration tests, and on-orbit tests.

A set of ground support equipment (GSE) was developed to support all levels of Beacon Receiver testing. Custom hardware in the GSE simulates the target signal as well as all interfaces between the Beacon Receiver and other MSX systems. The GSE simulates targets at various angles, frequencies, ranges, and signal dynamics so that system performance can be analyzed under typical and worst-case conditions. After integration of the Beacon Receiver with the spacecraft, the GSE will serve as a stimulator for Beacon Receiver health checks and for mission simulation tests. A workstation computer automates the GSE and permits analysis and recording of all results.

Brassboard model tests were performed at the module level for each subsystem, except for the DPU, which was tested using wire-wrapped breadboard models. These tests were conducted informally with each subsystem engineer responsible for developing the test procedures, overseeing the tests, and analyzing and documenting the results. System tests were performed at the brassboard level for all subsystems except for the antenna array. The system brassboard permitted testing the compatibility of

all subsystems with each other as well as with other spacecraft system brassboards.

Each flight electronics module was tested for electrical performance, and the results were compared to predicted or specified performance. All modules except the DPU were environmentally qualified prior to Beacon Receiver integration, including vibration testing in the APL Vibration Laboratory and thermal vacuum testing in the APL Space Simulation Laboratory. In addition, the DDS module underwent qualification tests to assess the performance over time of the GaAs devices and of the green tape hybrid substrate.<sup>5</sup> The antenna dish assemblies were assembled, aligned, and tuned. Acceptance tests were performed on purchased components, including the antenna array bench and the two DC-DC converter units. The antenna assembly deployment mechanism was tested at realistic on-orbit temperatures to verify reliable deployment. Qualification tests were performed to show that the pilot-tone distribution network would maintain channel-to-channel phase coherence over various temperatures.

The boresight and calibration tests were performed using the APL Space Department 75-m outdoor antenna range. These tests and the baseline performance test are the only prelaunch system tests in which target beacon signals are radiated through space. For the tests, the target beacon system is simulated by a microwave signal generator and a 2.4-m source dish. The Beacon Receiver antenna assembly is mounted on the antenna range positioner, which allows it to be pointed at arbitrary offset angles relative to the source dish or spun about its axis. In preparation for testing, the alignment engineer defined an optical boresight for the Beacon Receiver and mounted a precision mirror normal to the boresight in the center of the array. During the test, the off-boresight angle was set for each measurement by locating a surveying theodolite a known distance from the target dish center and pointing the Beacon Receiver alignment mirror to within  $\pm 0.01^\circ$  of the theodolite axis. In this way, optically verified angles were derived for comparison with the Beacon Receiver reading, and the Beacon Receiver electrical array boresight was mapped into the optical boresight. Calibration factors were derived and programmed into the Beacon Receiver firmware to provide for automatic calibration in flight. (The software allows for overriding the calibrations with new parameters should the calibration change.) The calibration factors derived in this testing account for such problems as pilot-tone distribution network alignment, antenna array geometry, and antenna phase and gain response over frequency, field of view, and polarization. Figure 14 shows photographs of the Beacon Receiver undergoing the boresight and calibration testing. The testing showed that the worst-case tested conditions accounted for azimuth and elevation errors (one standard deviation) of less than  $\pm 0.04^\circ$ . Analysis indicates that even when additional error sources (such as thermal dish, feed, cable, or hinge distortion and multipath effects from the top of the spacecraft structures) are included, the Beacon Receiver will still achieve the design specification of  $\pm 0.1^\circ \times \pm 0.1^\circ$ . Figure 15 shows the final calibrated results from the testing of a 2229.5-MHz beacon rotated in a  $2.5^\circ$  half angle cone





**Figure 14.** Flight hardware boresight calibration of the Beacon Receiver at the Space Department antenna range. **A.** Beacon Receiver antenna assembly mounted on the antenna range positioner tower. Assembled test and analysis team includes (L-R) R. K. Stilwell, M. L. Edwards, T. R. McKnight, C. R. Valverde, J. R. Jensen, R. F. Platte, J. T. Will, and C. C. DeBoy. **B.** T. R. McKnight conducts Beacon Receiver tests while R. F. Platte controls the Beacon Receiver via its ground support equipment and J. T. Will operates the antenna positioner. **C.** C. C. DeBoy uses a theodolite to boresight the Beacon Receiver at the desired angle offset from the simulated target beacon.

about the array optical boresight. In this figure, all results have been rotated and shifted back to the origin so that the points on the graph show errors. The small bias toward negative azimuth and elevation was found to be frequency dependent, but was consistent over all orientations of the Beacon Receiver at all angle offsets taken. This bias is believed to be caused by antenna range effects and represents an apparent shift of the source antenna phase center of less than 10 cm from the dish geometric center.

After calibration, the antenna assembly was environmentally qualified. The Beacon Receiver is currently being prepared for the baseline performance test. For this test, the Beacon Receiver will be returned to the antenna range to recheck the Beacon Receiver calibration and verify that the antenna array geometry did not change as a result of the antenna assembly qualification process. Afterwards, the main electronics assembly will be vibrated and tested in a thermal-vacuum chamber, and then the Beacon Receiver will be ready for integration with the MSX spacecraft.

During spacecraft integration, the Beacon Receiver will undergo standard electrical bonding and electrical interface compatibility checks. The interfaces will be verified at a higher level during mission simulations involving multiple systems and their stimulators. Health and readiness tests can be conducted using either the GSE as a stimulator or using a built-in self-test wherein the internally generated pilot tone is used as an RF stimulus. Compatibility with the MSX 2282.5-MHz communications downlink signal will be tested by turning on the MSX downlink transmitter and commanding the Beacon Receiver to track simulated targets near known spurious frequencies in the downlink signal.

The deployment of the antenna array will be verified on-orbit using both ground-based and orbital targets during the initial weeks after launch and periodically thereafter. In operation, the tracking processor system will perform the mapping of the Beacon Receiver boresight into the spacecraft coordinates. Compatibility with the MSX 2282.5-MHz communications downlink signal will be retested on-orbit. Operational readiness will be deter-



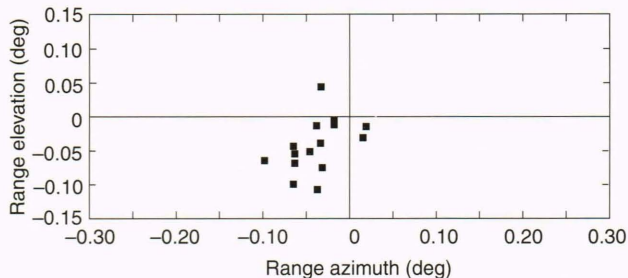


**Figure 15.** Beacon Receiver boresight and calibration test errors. The Beacon Receiver was aligned on a surveyor's theodolite 2.5° away from the center of the simulated beacon source antenna and then rolled with measurements taken at 45° and 30° increments. All results were rotated and shifted back to the origin so that the graph shows errors in (antenna) range coordinates. Beacon frequency = 2229.5 MHz.

mined using the built-in test that measures the level and phase of the pilot tone from each receiver channel.

### SUMMARY

A high-resolution angle-tracking instrument, the MSX S-band Beacon Receiver, has been developed to perform angle tracking of cooperative targets from space for the MSX program. The Beacon Receiver combines both amplitude- and phase-comparison monopulse techniques with an innovative real-time, on-board calibration scheme and extensive processing to provide high-precision angle

measurements over a large field of view with no grating-lobe ambiguities. The system is scheduled for delivery to the payload engineer for integration with the MSX spacecraft early in 1994.

### REFERENCES

- <sup>1</sup>Huebschman, R. K., and Pardoe, C. T., "The Midcourse Space Experiment Spacecraft," in *Proc. AIAA Aerospace Design Conf.*, AIAA92-077 (1992).
- <sup>2</sup>Sherman, S. M., *Monopulse Principles and Techniques*, Artech House (1984).
- <sup>3</sup>Stilwell, R. K., "Satellite Applications of the Bifilar Helix Antenna," *Johns Hopkins APL Tech. Dig.* **12**(1), 75-80 (1991).
- <sup>4</sup>Jablon, A. R., and Persons, D. F., "Thermal Distortion Analysis for Space-Based Monopulse Radar Antenna Array," in *Proc. RFEXPO West*, pp. 161-172 (1992).
- <sup>5</sup>Denissen, R. A., McCarty, T. A., Clatterbaugh, G. V., Chao, K., Mobley, S. J., Fraeman, M. E., Lohr, D. A., Trimble, W. C., and Valverde, C. R., "A GaAs DDS for Space Applications," *Government Microcircuits and Applications Conference Digest of Papers* **17**, 601-604 (1991).
- <sup>6</sup>Russo, A. A., and Clatterbaugh, C. V., "A Space-Based High-Speed Direct Digital Synthesizer Multichip Module Using Low-Temperature Co-Fired Ceramic," *Johns Hopkins APL Tech. Dig.* **14**(4), 324-332 (1993).
- <sup>7</sup>McKnight, T. R., and Valverde, C. R., "Signal Processing for a Space-Based Monopulse Radar," in *Proc. RFEXPO West*, pp. 137-160 (1992).
- <sup>8</sup>Harris, F. J., "On the Use of Windows for Harmonic Analysis with the Discrete Fourier Transform," *Proc. IEEE* **66**, 51-83 (1978).

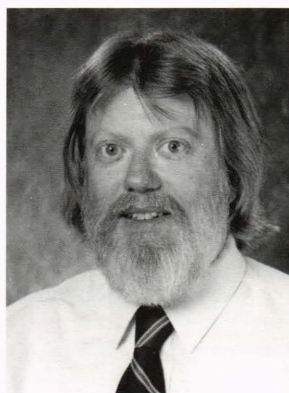
**ACKNOWLEDGMENTS:** The MSX S-band Beacon Receiver project has been a team effort requiring the talents and skills of many hardware and software engineers as well as supporting staff. The authors wish to acknowledge J. Robert Jensen, Robert F. Platte, Christopher C. DeBoy, John Daniels, David F. Persons, Steven R. Vernon, Guy V. Clatterbaugh, Taunya A. McCarty, Jonathan C. Barnett, Stanley B. Cooper, John L. MacArthur, Ernest Byron, and Paul C. Marth for their contributions. Max R. Peterson, M. Lee Edwards, Joseph L. Abita, Richard K. Huebschman, and C. Thompson Pardoe are acknowledged for their support. This work is sponsored by the Ballistic Missile Defense Organization / Sensor Technology Directorate (BMDO/DTS) under contract N00039-91-C-0001 from the Department of the Navy Space and Naval Warfare Systems Command.

### THE AUTHORS



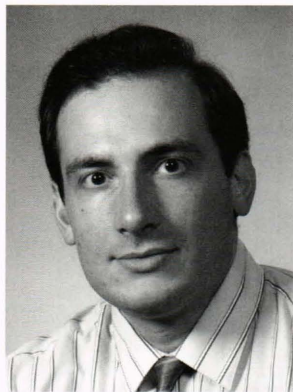
CARLOS R. VALVERDE is currently head of the Sensors Section of the Microwave and RF Systems Group of the APL Space Department and a member of the Senior Professional Staff. He earned a B.S.E.E. from Washington University in St. Louis in 1979 and came to APL as a member of the 1979 Associate Staff Training Program. He subsequently joined the Space Department Satellite Communications Group, where he applied computer and signal processing technologies to satellite communications problems. Since 1989, he has been the lead engineer for the

MSX S-band Beacon Receiver, which is a high-precision space-based microwave angle-tracking system for acquiring and tracking MSX targets.



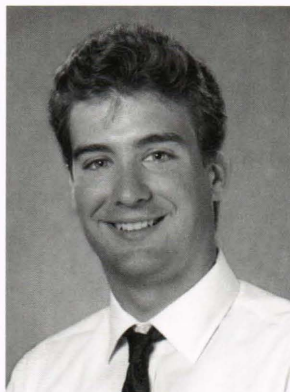
ROBERT K. STILWELL received his B.S. degree in electrical engineering from Kansas State University in 1973 and his M.S. degree from The Johns Hopkins University in 1976. Since joining APL in 1973, he has been involved in the design, development, and testing of various types of antennas that have flown on more than twenty satellites. He has also been concerned with ground-based antennas and has contributed to numerous Space Department studies. Mr. Stilwell is the supervisor of the Antenna Systems Section of the Microwave and RF Systems Group.





ALBERTO A. RUSSO received a B.S.E.E. in 1983 and an M.S.E.E. in 1987 from the George Washington University. Before joining APL in 1988, he was employed by COMSAT, where he was a senior communications systems engineer. At APL he is a Senior Staff member in the Microwave and RF Systems Group of the Space Department, where he specializes in RF design and satellite communications technology. Mr. Russo teaches a graduate course in satellite communications systems and also conducts a monthly seminar on communications technology

topics at The Johns Hopkins University G.W.C. Whiting School of Engineering.



THOMAS R. McKNIGHT received a B.S. in electrical engineering from the University of Maryland in 1985, and an M.S. in electrical engineering from The Johns Hopkins University in 1989. He began his career at APL in 1985 as a design engineer developing Global Positioning System receiver hardware and software. More recently, Mr. McKnight has worked on the development of hardware, software, and algorithms for the MSX S-band Beacon Receiver digital processor. Prior to this, he developed signal processing algorithms for the detection of speech in noise, and for the

analysis of signal returns from the laser radar vibration sensor. Before joining APL, he designed electronic hardware for radio proximity fuzes at the Harry Diamond Laboratories.